Article

Developmental Cell

Lrig2 Negatively Regulates Ectodomain Shedding of Axon Guidance Receptors by ADAM Proteases

Graphical Abstract

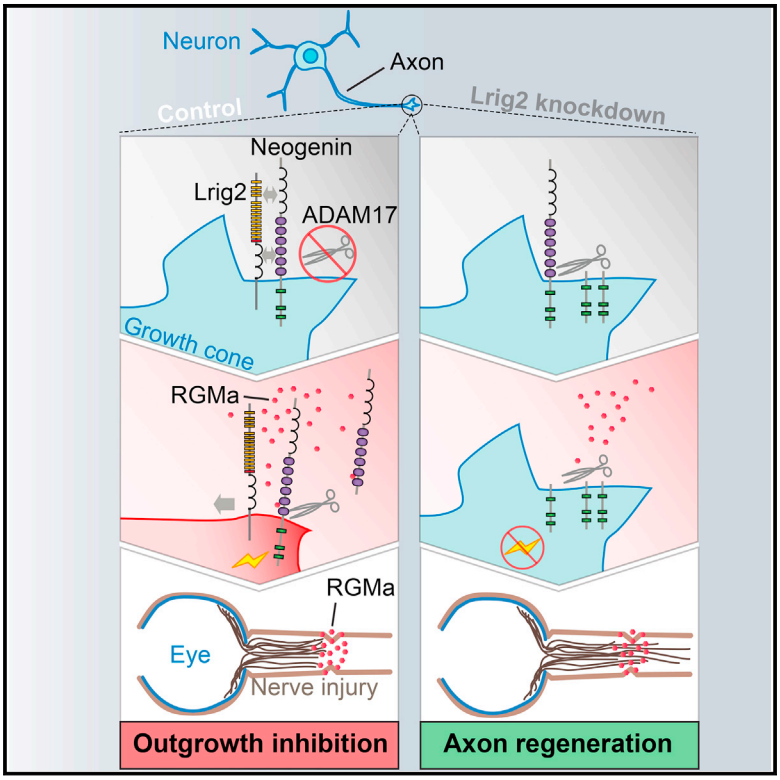

Authors

Susan van Erp,
Dianne M.A. van den Heuvel,
Yuki Fujita, ..., Christian Siebold,
Toshihide Yamashita,
R. Jeroen Pasterkamp

Correspondence

r.j.pasterkamp@umcutrecht.nl

In Brief

How proteolytic cleavage of cell-surface proteins is controlled in neurons is incompletely understood. Van Erp and van den Heuvel et al. show that Lrig2 negatively regulates ADAM17-mediated ectodomain shedding of the guidance receptor Neogenin. This process is required for proper neuron migration during embryonic development and during axon regeneration.

Highlights

- Lrig2 negatively regulates ectodomain shedding of Neogenin by ADAM17
- RGMa inhibits Lrig2-Neogenin binding, allowing ADAM17-mediated cleavage of Neogenin
- Lrig2 controls neuron migration, and Lrig2 knockdown improves axon regeneration
- Lrig2 inhibits ectodomain shedding of multiple, distinct ADAM17 substrates

van Erp et al., 2015, Developmental Cell *35*, 537–552
December 7, 2015
http://dx.doi.org/10.1016/j.devcel.2015.11.008

CellPress

Developmental Cell
Article

Lrig2 Negatively Regulates Ectodomain Shedding of Axon Guidance Receptors by ADAM Proteases

Susan van Erp,[1,7] Dianne M.A. van den Heuvel,[1,7] Yuki Fujita,[2] Ross A. Robinson,[3] Anita J.C.G.M. Hellemons,[1] Youri Adolfs,[1] Eljo Y. Van Battum,[1] Anna M. Blokhuis,[1] Marijn Kuijpers,[4] Jeroen A.A. Demmers,[5] Håkan Hedman,[6] Casper C. Hoogenraad,[4] Christian Siebold,[3] Toshihide Yamashita,[2] and R. Jeroen Pasterkamp[1,*]
[1]Department of Translational Neuroscience, Brain Center Rudolf Magnus, University Medical Center Utrecht, 3584 CG Utrecht, the Netherlands
[2]Department of Molecular Neuroscience, Graduate School of Medicine, Osaka University 2-2, Yamadaoka, Suita, Osaka 565-0871, Japan
[3]Division of Structural Biology, Wellcome Trust Centre for Human Genetics, University of Oxford, Oxford OX3 7BN, UK
[4]Cell Biology, Faculty of Science, Utrecht University, 3584 CH Utrecht, the Netherlands
[5]Proteomics Centre and Department of Cell Biology, Erasmus University Medical Centre, Dr Molewaterplein 50, 3015 GE Rotterdam, the Netherlands
[6]Oncology Research Laboratory, Department of Radiation Sciences, Umeå University, 90187 Umeå, Sweden
[7]Co-first author
*Correspondence: r.j.pasterkamp@umcutrecht.nl
http://dx.doi.org/10.1016/j.devcel.2015.11.008

SUMMARY

Many guidance receptors are proteolytically cleaved by membrane-associated metalloproteases of the ADAM family, leading to the shedding of their ectodomains. Ectodomain shedding is crucial for receptor signaling and function, but how this process is controlled in neurons remains poorly understood. Here, we show that the transmembrane protein Lrig2 negatively regulates ADAM-mediated guidance receptor proteolysis in neurons. Lrig2 binds Neogenin, a receptor for repulsive guidance molecules (RGMs), and prevents premature Neogenin shedding by ADAM17 (TACE). RGMa reduces Lrig2-Neogenin interactions, providing ADAM17 access to Neogenin and allowing this protease to induce ectodomain shedding. Regulation of ADAM17-mediated Neogenin cleavage by Lrig2 is required for neurite growth inhibition by RGMa in vitro and for cortical neuron migration in vivo. Furthermore, knockdown of Lrig2 significantly improves CNS axon regeneration. Together, our data identify a unique ligand-gated mechanism to control receptor shedding by ADAMs and reveal functions for Lrigs in neuron migration and regenerative failure.

INTRODUCTION

Leucine-rich repeats and immunoglobulin-like domains (Lrig) proteins are unique transmembrane proteins with an extracellular domain containing leucine-rich repeats (LRRs) and immunoglobulin-like (Ig-like) domains and a cytosolic region with no apparent homology to other proteins (Figure 1A). The Lrig family contains three vertebrate members, Lrig1 (Lig1), Lrig2, and Lrig3, while *Drosophila* and *Caenorhabditis elegans* each contain a single Lrig gene (Guo et al., 2004). Lrig1 is best characterized at the functional level and controls the activity of several growth factor receptors (e.g., Gur et al., 2004; Laederich et al., 2004; Ledda et al., 2008). Lrig1 deficiency in mice leads to a variety of phenotypes, including excess intestinal stem cell proliferation, tumor formation, impaired auditory responses, and psoriasis-like hyperplasia (Del Rio et al., 2013; Page et al., 2013; Powell et al., 2012; Suzuki et al., 2002; Wong et al., 2012). In addition, Lrig1 has been described as a tumor suppressor in humans and is associated with tumor growth and patient survival (Lindquist et al., 2014). Unfortunately, our understanding of the function and mechanism of action of other Lrigs is rather rudimentary. Further, despite prominent neuronal expression of Lrigs, how these proteins contribute to nervous system development or function is poorly understood.

Here, we show that Lrig2 controls the proteolytic processing of axon guidance receptors. During embryonic development, axon guidance proteins provide instructive signals for growing axons and migrating neurons and are detected by cell-surface receptors at the growth cone (Kolodkin and Pasterkamp, 2013). Many axon guidance receptors are proteolytically cleaved at their juxta-membrane region by membrane-associated metalloproteases of the ADAM (A disintegrin and metalloprotease) family, leading to the shedding of their ectodomains. This shedding is required for proper axon guidance and controls receptor levels, activation, and the disassembly of ligand-receptor complexes (Bai and Pfaff, 2011). Despite these important roles, how the neuronal effects of ADAMs are controlled to regulate axon guidance receptor signaling remains incompletely understood. For example, shedding of Neogenin, a receptor for repulsive guidance molecule a (RGMa) (Matsunaga et al., 2004; Monnier et al., 2002; Rajagopalan et al., 2004) by ADAM17 desensitizes axons to RGMa, but how this cleavage event is initially prevented to allow cleavage only after ligand binding is unknown (Okamura et al., 2011). Thus, unidentified regulatory mechanisms are in place to control ADAM17-mediated Neogenin cleavage in neurons.

In this study, we identify Lrig2 as a binding partner of Neogenin and show that Lrig2 prevents the premature shedding of Neogenin by ADAM17 in an RGMa-dependent manner. This regulatory

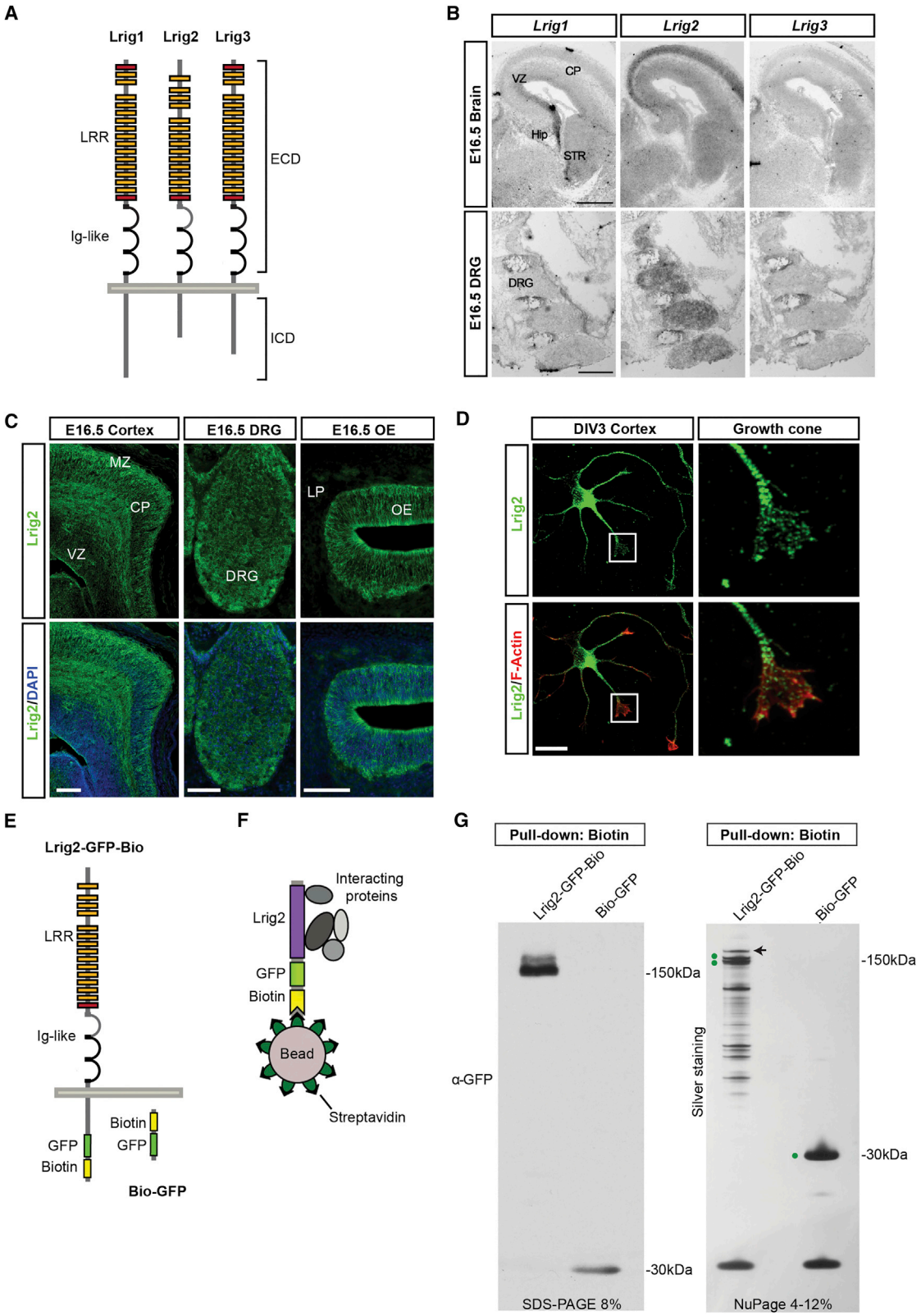

Figure 1. Expression of Lrig2 during Neural Development

(A) The Lrig family in vertebrates. ECD, extracellular domain; ICD, intracellular domain; Ig, immunoglobulin; LRR, leucine-rich repeat.

(B) In situ hybridization for *Lrig1*, *Lrig2*, or *Lrig3* on coronal (upper panels) and sagittal (lower panels) sections from E16.5 mouse embryos. CP, cortical plate; DRG, dorsal root ganglion; Hip, hippocampus; STR, striatum; VZ, ventricular zone.

(legend continued on next page)

mechanism is required for the axon growth inhibitory effects of RGMa-Neogenin signaling in vitro. In line with this observation and with the regeneration-inhibiting effect of RGMa (Hata et al., 2006), knockdown of Lrig2 significantly promotes optic nerve regeneration in vivo. Finally, we show that regulation of ADAM17-mediated cleavage of Neogenin by Lrig2 controls neuronal migration in the embryonic cortex in vivo. These data reveal a neuronal role for Lrigs and unveil a previously uncharacterized mechanism in ADAM regulation that prevents premature receptor cleavage while retaining ligand responsiveness.

RESULTS

Expression of Lrigs in the Developing Nervous System

How Lrig proteins contribute to CNS development remains unexplored. To address this question, we determined neural Lrig expression patterns using in situ hybridization. All three *Lrigs* were detected in the developing mouse brain and spinal cord, displaying clearly distinct patterns of expression (Figures 1B and S1). Expression of *Lrig1* was strong in the ventricular zones of the embryonic nervous system, while at postnatal day 9 (P9), *Lrig1* was detected in differentiated neurons. *Lrig2* and *Lrig3* displayed overlapping patterns of expression, but *Lrig2* was more widespread and several structures showed *Lrig2* but no *Lrig3* labeling (Figures 1B and S1). This pattern of neural Lrig expression was confirmed by immunohistochemistry at embryonic day E16.5. Lrig1 prominently labeled ventricular regions. Lrig2 was strongly expressed throughout the brain, while many Lrig2-positive areas did not show Lrig3 labeling (Figures 1C, S2, S3A, and S3B). Of all three Lrigs, Lrig2 was most abundantly expressed in post-mitotic neurons. Therefore, to begin to dissect the role of Lrigs during CNS development, we focused on Lrig2.

Lrig2 Binds the Guidance Receptor Neogenin in Neurons

Further characterization of Lrig2 expression by immunocytochemistry on dissociated cortical neurons revealed strong expression in the cell body and punctate staining in neurites and growth cones (Figure 1D), suggesting a role for Lrig2 in axon growth and guidance. As a first step toward determining the function of Lrig2, we used a biotin-streptavidin-based purification method to identify Lrig2-interacting proteins (Figures 1E and 1F) (Groen et al., 2013). This system allowed for highly specific pull-down of biotinylated full-length Lrig2 using streptavidin-coated beads (Figure 1G). Silver staining revealed multiple specific Lrig2-interacting proteins (Figure 1G), and mass spectrometry analysis of the pull-down samples identified many proteins that were present specifically in Lrig2-GFP-Bio complexes. Interestingly, several of the candidate interactors had reported roles in axon growth and guidance, cytoskeletal organization, and intracellular transport (Table S1).

One of the candidate interactors was Neogenin, a cell-surface receptor for RGMs, bone morphogenetic proteins (BMPs), and Netrins. In the nervous system, Neogenin has been best characterized as a growth cone receptor for RGMa (Figure 2A). To examine whether Lrig2 contributes to RGMa-Neogenin signaling, we first confirmed the interaction between Neogenin and Lrig2 in HEK293 cells transiently overexpressing full-length Neogenin (NeoFL-GFP-Bio) or the Neogenin intracellular domain (ICD; Bio-GFP-NeoICD). Endogenous Lrig2 was detected following pull-down of NeoFL-GFP-Bio, but not of Bio-GFP-NeoICD. In contrast, Myosin-X, which is known to interact with the Neogenin ICD (Zhu et al., 2007), co-precipitated with full-length Neogenin and the Neogenin ICD (Figure 2B). Next, we performed co-immunoprecipitation experiments from N1E-115 neuronal cell lysates and P0 brains using Neogenin- and Lrig2-specific antibodies. Endogenous Lrig2 co-precipitated with endogenous Neogenin from neuronal cell lysates, and vice versa (Figures 2C, 2D, and S3C). Similarly, pull-down of Neogenin from P0 brain lysates resulted in co-precipitation of Lrig2 (Figure 2E).

The interaction between Lrig2 and Neogenin in brain tissue suggests that these proteins co-localize in neurons. Indeed, immunohistochemistry revealed that at E16.5, the majority of neurons in the cortex and a subset of cortical axons in the external capsule co-expressed Neogenin and Lrig2 (Figures 2F–2K). Furthermore, immunostaining of dissociated cortical neurons for Neogenin and Lrig2 overlapped, but vesicular structures expressing Neogenin, but not Lrig2, and vice versa, were also observed (Figures 2L–2Q). Together, these results show that Lrig2 and Neogenin interact and partly co-localize in neurons.

Neogenin and Lrig2 Interact through Their Extracellular Domains

To further define the interaction between Neogenin and Lrig2, a series of truncation mutants was generated (Figures S4A and S4B) and used in pull-down assays. Lrig2 constructs containing the LRR and/or Ig-like domains showed binding to Neogenin, but binding of the Lrig2 Ig-like region (Lrig2-ΔLRR) to Neogenin was more robust as compared to Lrig2-LRR-Neogenin binding (Figures S4C and S4E). The Neogenin ICD region did not interact with Lrig2 (Figure 2B), but Neogenin proteins containing the Ig-like and/or fibronectin type III (FN) regions bound Lrig2 (Figures S4D and S4F). To further dissect these interactions, we carried out surface plasmon resonance (SPR) equilibrium binding experiments. Our analysis revealed that the full-length ectodomain of Lrig2 (Lrig2-ECD) bound to full-length Neogenin ectodomain

(C) Immunohistochemistry for Lrig2 in coronal sections of an E16.5 mouse embryo (green). DAPI in blue (lower panels). LP, lamina propria; MZ, marginal zone; OE, olfactory epithelium.

(D) E14.5 mouse cortical neuron cultures analyzed at 3 days in vitro (DIV) by immunocytochemistry using anti-Lrig2 antibodies. Phalloidin staining in red. Right panels show a higher magnification of the boxed areas in the left panels.

(E) Biotin- and GFP-tagged Lrig2 construct used in the pull-down experiments in (G).

(F) Biotin-streptavidin pull-down assay. Lrig2-GFP-Bio or Bio-GFP are biotinylated by the co-transfected biotin ligase BirA and purified by precipitation using streptavidin-coated beads, along with interacting proteins. Purple region indicates full-length Lrig2.

(G) Streptavidin pull-down assays on lysates of HEK293 cells co-expressing Bio-GFP or Lrig2-GFP-Bio and BirA. Proteins bound to streptavidin beads were analyzed by western blotting using anti-GFP antibodies (left panel). The same samples were separated on a gradient gel followed by silver staining (right panel). Dots indicate Lrig2-GFP-Bio and Bio-GFP, and arrow indicates endogenous Neogenin.

Scale bars represent 500 μm (B), 100 μm (C), and 20 μm (D). See also Figures S1–S3 and Table S1.

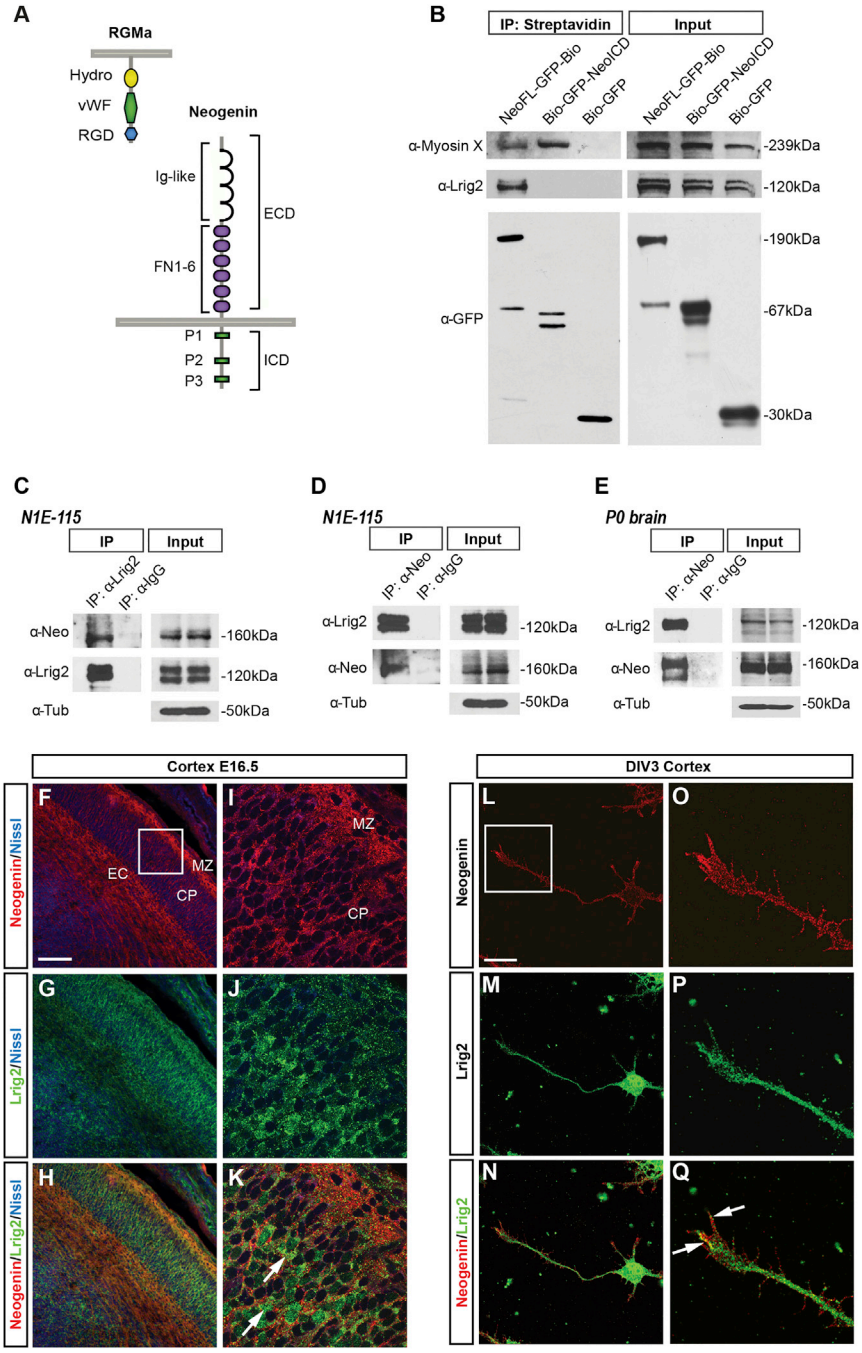

Figure 2. Lrig2 Binds and Co-localizes with the RGMa Receptor Neogenin in Neurons

(A) Neogenin and its ligand RGMa (repulsive guidance molecule a). ECD, extracellular domain; FN, fibronectin type III; Hydro, hydrophobic domain; ICD, intracellular domain; Ig, immunoglobulin; RGD, Arg-Gly-Asp; vWF, partial von Willebrand factor type D.

(B) Streptavidin pull-down assays were performed on lysates of HEK293 cells co-transfected with the indicated constructs and BirA. Co-immunoprecipitated proteins were analyzed by western blotting using the indicated antibodies. Myosin X is a known Neogenin interactor.

(C and D) Lysates of N1E-115 cells were immunoprecipitated with anti-IgG (control), anti-Lrig2 (C), or anti-Neogenin (D) antibodies. The immunoprecipitates were analyzed with the indicated antibodies. Figure S3C shows full-size western blots.

(E) P0 mouse brain lysate was immunoprecipitated with anti-IgG and anti-Neogenin antibodies. The precipitates were analyzed with the indicated antibodies. Figure S3C shows full-size western blots.

(F–K) Immunohistochemistry for Neogenin (red) and Lrig2 (green) on E16.5 coronal mouse brain sections. (I)–(K) show higher magnifications of the boxed area in (F). Nissl is in blue. Arrows indicate co-expression of Lrig2 and Neogenin in cortical neurons. CP, cortical plate; EC, external capsule; MZ, marginal zone.

(L–Q) Immunocytochemistry for Neogenin (red) and Lrig2 (green) on E14.5 dissociated cortical neurons at DIV3. (O)–(Q) show higher magnifications of the boxed area in (L). Arrows indicate areas of co-expression.

All data represent at least three independent experiments. Scale bars represent 100 μm (F–K) and 20 μm (L–Q). See also Figure S3C.

(Neo-ECD) as well as Neogenin FN1–6 (Neo-FN1–6), but not to the Neo Ig1–4 domains (Neo-IG1–4) (Figure S4G). Lrig2-IG1–3 bound Neo-ECD and Neo-FN1–6, but Lrig2-LRR-IG1 did not show any binding to Neo-ECD (Figures S4H and S4I). This suggests that the two membrane-proximal Lrig2 Ig-like domains (IG2-3) and the six membrane-proximal Neogenin FN domains form the major interaction site in the Neogenin-Lrig2 complex. We had previously shown that the Neo-FN5-6 domains are the key interaction site for all human RGM family members (Bell et al., 2013). Interestingly, we observed binding in low micromolar range for Lrig2-IG1–3:Neo-FN5-6 (Figure S4J), but no binding for Lrig2-LRR-IG1:Neo-FN5-6 (Figure S4K). Finally, COS-7 cell binding assays were performed to determine whether the Neogenin ligand RGMa binds Lrig2. Strong binding of alkaline phosphatase (AP)-tagged RGMa (RGMa-AP) was observed in Neogenin$^+$, but not Lrig2$^+$, cells (Figure S4L). Together, our data indicate that the membrane-proximal Neo FN5-6 domains are crucial for Lrig2 binding and that RGMa binds Neogenin, but not Lrig2 (Figure S4M).

Lrig2 Is Required for RGMa-Neogenin-Mediated Signaling and Neurite Growth Inhibition

Binding of RGMa to Neogenin induces growth cone collapse and neurite growth inhibition. To determine whether Lrig2 is required for these effects, we knocked down Lrig2 in dissociated cortical neurons and performed growth cone collapse and CHO layer assays. Acute exposure of cortical neurons to RGMa induced growth cone collapse, but this effect was not observed following

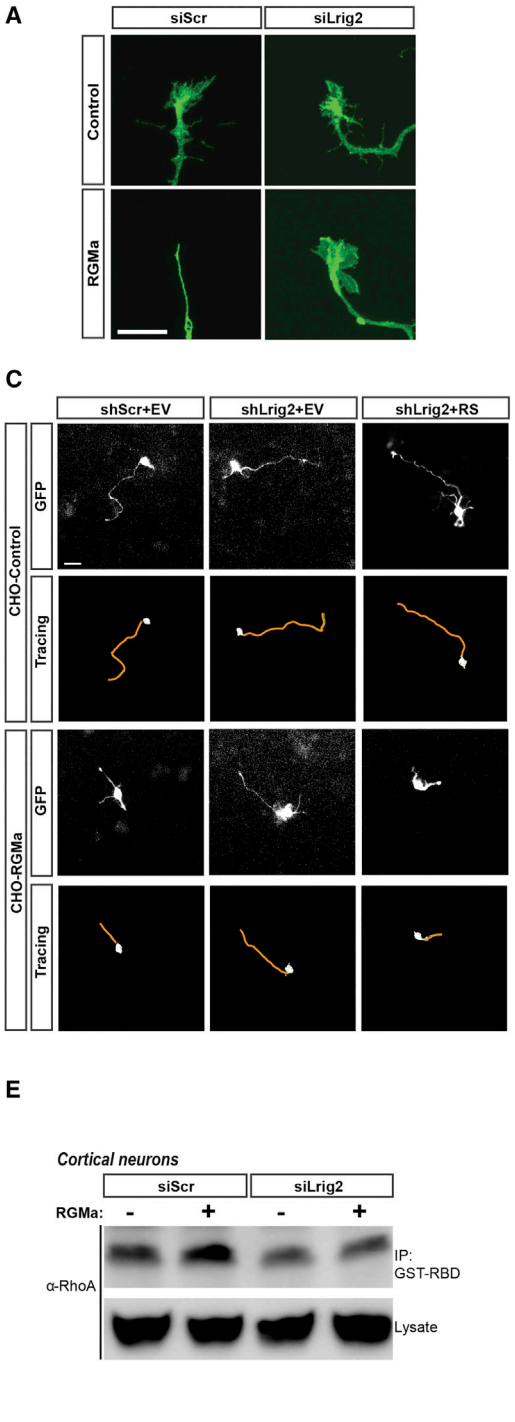

Figure 3. Lrig2 Is Required for RGMa-Induced Neurite Growth Inhibition and Signaling

(A) Immunocytochemistry for GFP in growth cones. Dissociated P0 cortical neurons were transfected with GFP vector and siRNAs (siScr or siLrig2) and exposed to RGMa ligand or control at 3 DIV.

(B) Graph shows percentage of growth cone collapse in RGMa-stimulated and control neurons. n = 2 experiments, >100 neurons per condition per experiment. *p < 0.05, Student's t test.

(C) Dissociated E14.5 cortical neurons were electroporated with GFP vector and combinations of the indicated vectors and grown on confluent CHO cell layers. RS is a rescue construct that is not targeted by shLrig2. At 4 DIV, cultures were fixed and immunostained with anti-GFP antibodies. Lower panels show tracing of the longest neurite in each example. EV, empty vector.

(D) Quantification of neurite length in cultures as in (C). Graphs show average length of the longest neurite normalized to control (shScr+EV on CHO-Control cells). n = 3 experiments, >50 neurons per condition per experiment. *p < 0.05, two-way ANOVA.

(E) E18 cortical neurons electroporated with siScr or siLrig2 were incubated with 2 μg/ml RGMa or control protein (BSA) at DIV3. Cell lysates were subjected to active RhoA pull-down assays, and cell lysates and pull-down samples were analyzed by western blotting using anti-RhoA antibodies.

(F) Quantification of band intensities in experiments as shown in (E). Signals from active RhoA bands were compared to those of total RhoA in each lane. Results are shown as fold change relative to control. *p < 0.05, one-way ANOVA followed by Tukey-Kramer's test.

All data are presented as means (of three or more independent experiments) ± SEM. Scale bars represent 10 μm (A) and 50 μm (C). See also Figures S5A–S5E.

Lrig2 knockdown (Figures 3A, 3B, and S5A–S5C). CHO assays, in which neurons are plated on a confluent layer of RGMa-expressing or control CHO cells (CHO-RGMa or CHO-Control), are used to study the neurite growth inhibitory effect of RGMa. Dissociated E14.5 mouse cortical neurons were electroporated with expression vectors containing shLrig2 or scrambled control small hairpin RNA (shRNA) (shScr) in combination with GFP and either empty vector or Lrig2-RS, a rescue construct that is not targeted by shLrig2 (Figures S5A–S5D). Neurite outgrowth from cortical neurons electroporated with shScr and empty vector (EV) was significantly reduced on CHO-RGMa as compared to CHO-Control cells (Figures 3C and 3D). However, knockdown of Lrig2 significantly reduced RGMa's inhibitory effect. Co-electroporation of shLrig2 and Lrig2-RS restored the sensitivity of neurites to RGMa, while electroporation of Lrig2-RS alone had no effect (Figures 3C and 3D). Thus, Lrig2 is required for RGMa-induced growth cone collapse and neurite growth inhibition.

Binding of RGMa to Neogenin induces activation of RhoA (Conrad et al., 2007; Hata et al., 2009). To query a role for Lrig2 in RGMa-dependent RhoA activation, Lrig2 was knocked down in mouse cortical neuron cultures and Rho activation was determined by affinity precipitation of GTP-bound RhoA. As reported previously, addition of 2 μg/ml RGMa for 15 min to cultures electroporated with control small interfering RNAs (siRNAs) (siScr)

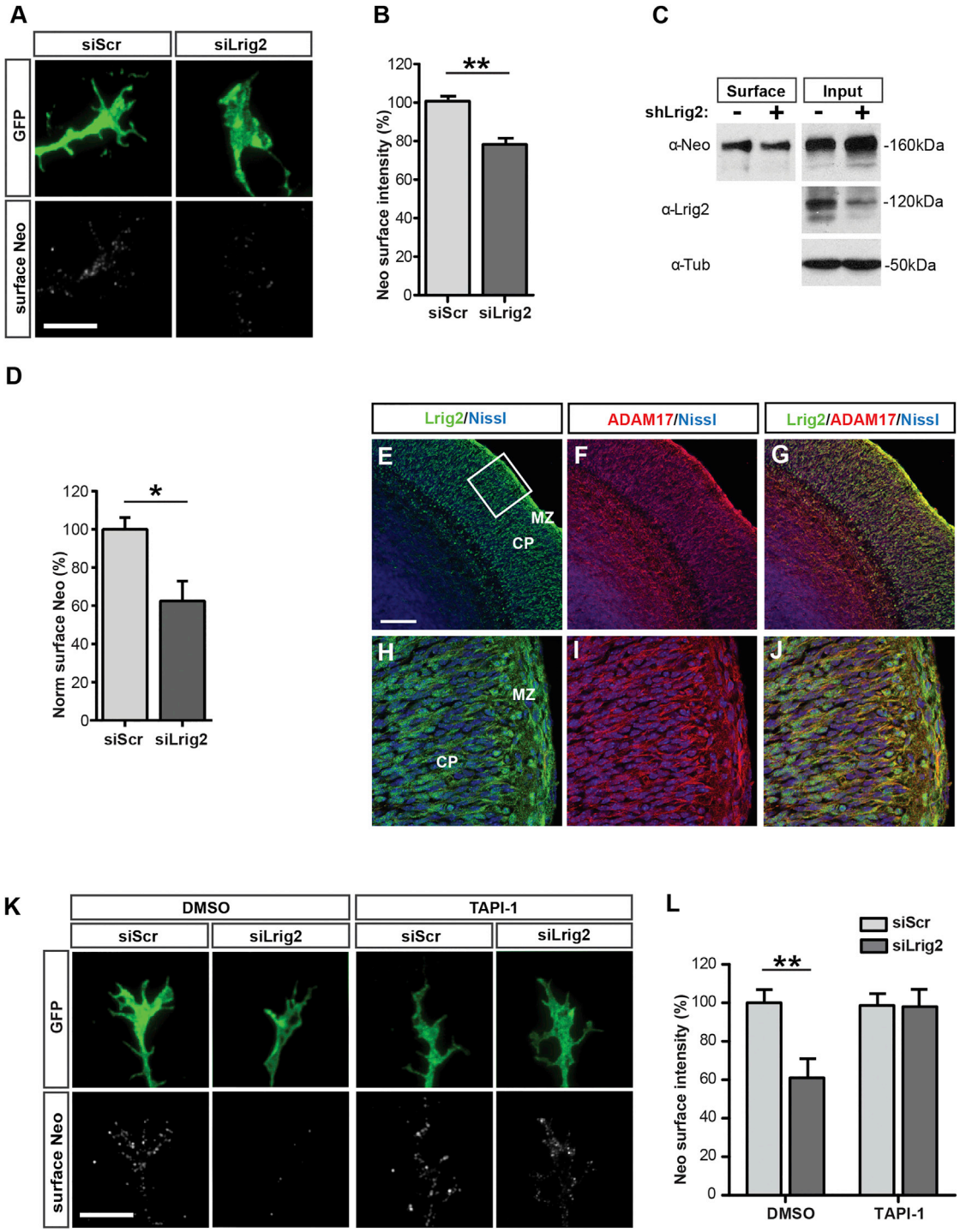

Figure 4. Lrig2 Regulates Neogenin Cell-Surface Expression at the Growth Cone

(A) Immunocytochemistry for intracellular GFP and cell-surface Neogenin expression in E14.5 cortical neuron growth cones transfected with siRNAs at 1 DIV and analyzed at 3 DIV.

(B) Quantification of growth cone fluorescent intensity as in (A). Data are normalized to siScr control. n = 3 experiments, >60 growth cones per condition per experiment. **$p < 0.01$, Student's t test.

(C) Endogenous surface proteins of N1E-115 cells transfected with pSuper-shScr or pSuper-shLrig2 were biotinylated on ice. Biotin-labeled surface proteins were pulled down using streptavidin-coated beads and subjected to western blotting.

(D) Quantification of band intensities as in (C). Neogenin surface levels are normalized to control. *$p < 0.05$, Student's t test.

(E–J) Immunohistochemistry for Lrig2 (green) and ADAM17 (red) in E16.5 coronal sections. (H)–(J) show higher magnifications of the boxed area in (E). Nissl is in blue. CP, cortical plate; MZ, marginal zone.

(legend continued on next page)

led to a ~2-fold increase in Rho activity. No RGMa-induced increase in Rho activity was observed following knockdown of Lrig2 (siLrig2; Figures 3E, 3F, and S5E). Thus, Lrig2 is required for signaling downstream of RGMa-Neogenin.

Lrig2 Regulates Neogenin Cell-Surface Expression

The next question we addressed was how Lrig2 influences RGMa-Neogenin signaling. A well-characterized effect of Lrigs is their ability to induce receptor ubiquitination and degradation. However, knockdown of Lrig2 did not change Neogenin protein levels in total neuronal cell lysates or Neogenin expression in primary cortical neurons (Figures S6A–S6C). Other previously reported effects of Lrigs, such as lipid raft recruitment, were also unchanged for Neogenin following Lrig2 knockdown (data not shown).

The cell-surface levels of axon guidance receptors are tightly controlled to dictate signaling duration, magnitude, and spatial activity. Therefore, we next explored the effect of Lrig2 on Neogenin cell-surface expression. Dissociated cortical neurons were transfected at DIV1 with siRNAs together with GFP and immunolabeled with antibodies against Neogenin at DIV3 under non-permeabilizing conditions. A significant decrease in Neogenin surface intensity was observed in neurons transfected with siLrig2 as compared to siScr (Figures 4A and 4B). In addition, cell-surface biotin labeling experiments in neuronal cells demonstrated a reduction in Neogenin cell-surface expression following Lrig2 knockdown (Figures 4C and 4D). These data unveil a role for Lrig2 in the regulation of Neogenin cell-surface expression.

Lrig2 Negatively Regulates ADAM17-Mediated Cleavage of Neogenin

Both Neogenin and Lrig2 are expressed in vesicular structures in the growth cone, which may represent exocytotic or endocytotic vesicles (Figures 2L–2Q). Defects in exocytosis or endocytosis could explain the reduction in Neogenin cell-surface expression observed following Lrig2 knockdown. However, Lrig2 knockdown did not affect internalization of Neogenin as assessed by anti-Neogenin antibody internalization and cell-surface biotinylation experiments (Figures S6D–S6G). In addition, fluorescence recovery after photobleaching (FRAP) of pHLuorin-Neogenin was intact following Lrig2 knockdown (Figures S5F, S6H, and S6I). These data suggest that exo-endocytic recycling of Neogenin is independent of Lrig2.

ADAM17 cleaves and sheds the Neogenin ECD at the growth cone membrane and desensitizes cortical neurons to the repulsive effects of RGMa (Goldschneider et al., 2008; Okamura et al., 2011). Therefore, a possible explanation for the effect of Lrig2 on Neogenin cell-surface expression is that Lrig2 negatively regulates Neogenin ectodomain shedding. If so, Lrig2 knockdown would induce enhanced shedding and reduce Neogenin cell-surface expression. To test this hypothesis, we first confirmed that Lrig2 and ADAM17 co-localize in embryonic cortical neurons (Figures 4E–4J). Next, dissociated cortical neurons were transfected with siRNAs and cultured in the presence of TAPI-1, an inhibitor of ADAM17 and other metalloproteases, or vehicle. Knockdown of Lrig2 induced a significant decrease in cell-surface Neogenin expression, but this effect was not observed in the presence of TAPI-1 or following ADAM17 knockdown (Figures 4K, 4L, and 6H). This suggests that Lrig2 normally negatively regulates Neogenin shedding by ADAM17. To further implicate Lrig2 in Neogenin shedding, HEK293 cells were transfected with Neogenin-GFP-Bio and a combination of ADAM17 and/or Lrig2 expression constructs. ADAM17-mediated Neogenin cleavage was reduced by co-transfection of full-length Lrig2 or the Lrig2 ECD, but not by the Lrig2 ICD (Figures 5A, 5B, and 5D). These data show that the Lrig2 ECD blocks ADAM17-induced cleavage of Neogenin.

The activity of ADAM17 is regulated through extra- and intracellular mechanisms. Lrig2 binds the ECD of Neogenin, and the Lrig2 ECD is sufficient to block cleavage of Neogenin. This suggests that Lrig2 is an extracellular regulator of ADAM17. To provide further support for this model, we incubated lysates of HEK293 cells transfected with Neogenin-GFP-Bio and empty vector (EV) or Lrig2-FL with recombinant ADAM17 extracellular domain (r-ADAM17). Addition of r-ADAM17, but not other ADAMs such as ADAM9 or ADAM10 (Figure S6J), enhanced Neogenin cleavage. As predicted, this effect was not observed in the presence of Lrig2 (Figures 5C and 5E). Because Lrig2 and ADAM17 interact with the Neogenin ECD, we hypothesized that Lrig2 may interfere with ADAM17-Neogenin binding. Pull-down of Neogenin from neuronal membrane fractions resulted in co-precipitation of Lrig2 and confirmed that Lrig2 and Neogenin interact at the membrane where ADAM17-mediated cleavage occurs (Figure 5F). Furthermore, Lrig2 effectively reduced binding between Neogenin and ADAM17 in ELISAs (Figure 5G). These data suggest that binding of Lrig2 to Neogenin prevents this guidance receptor from interacting with ADAM17.

We next asked how binding of Lrig2 to Neogenin is regulated to allow Neogenin shedding. To address this question, neuronal cells were treated with RGMa-His in combination with TAPI-1 or DMSO vehicle. Conditioned medium was collected from the cells and immunoprecipitated using antibodies directed against the Neogenin ECD. Incubation with RGMa-His increased the amount of Neogenin ECD in the medium, and this effect was nullified by addition of TAPI-1 (Figures 5H and 5I). These results suggest that ectodomain shedding of Neogenin is ligand (RGMa) dependent. A possible explanation for this result is that RGMa induces a reduction in the interaction between Lrig2 and Neogenin, providing ADAM17 access to Neogenin. In line with this model, Neogenin-Lrig2 binding was significantly reduced in the presence of RGMa, while Lrig2 and Neogenin levels were unaffected (Figures 5J and 5K). Finally, to examine whether regulation of shedding by Lrig2 contributes to RGMa-Neogenin signaling at the functional level, dissociated cortical neurons were electroporated with shLrig2 or shScr and cultured on

(K) Immunocytochemistry for intracellular GFP and cell-surface Neogenin expression in growth cones of E14.5 cortical neurons transfected with siRNAs at 1 DIV and cultured with vehicle (DMSO) or TAPI-1.

(L) Quantification of growth cone fluorescent intensity as in (K). Data were normalized to siScr control. n = 3 experiments, >60 growth cones per condition per experiment. **$p < 0.01$, Student's t test.

All data are presented as means (of three or more independent experiments) ± SEM. Scale bar represents 10 μm (A, E, and K). See also Figures S5E, S5F, and S6.

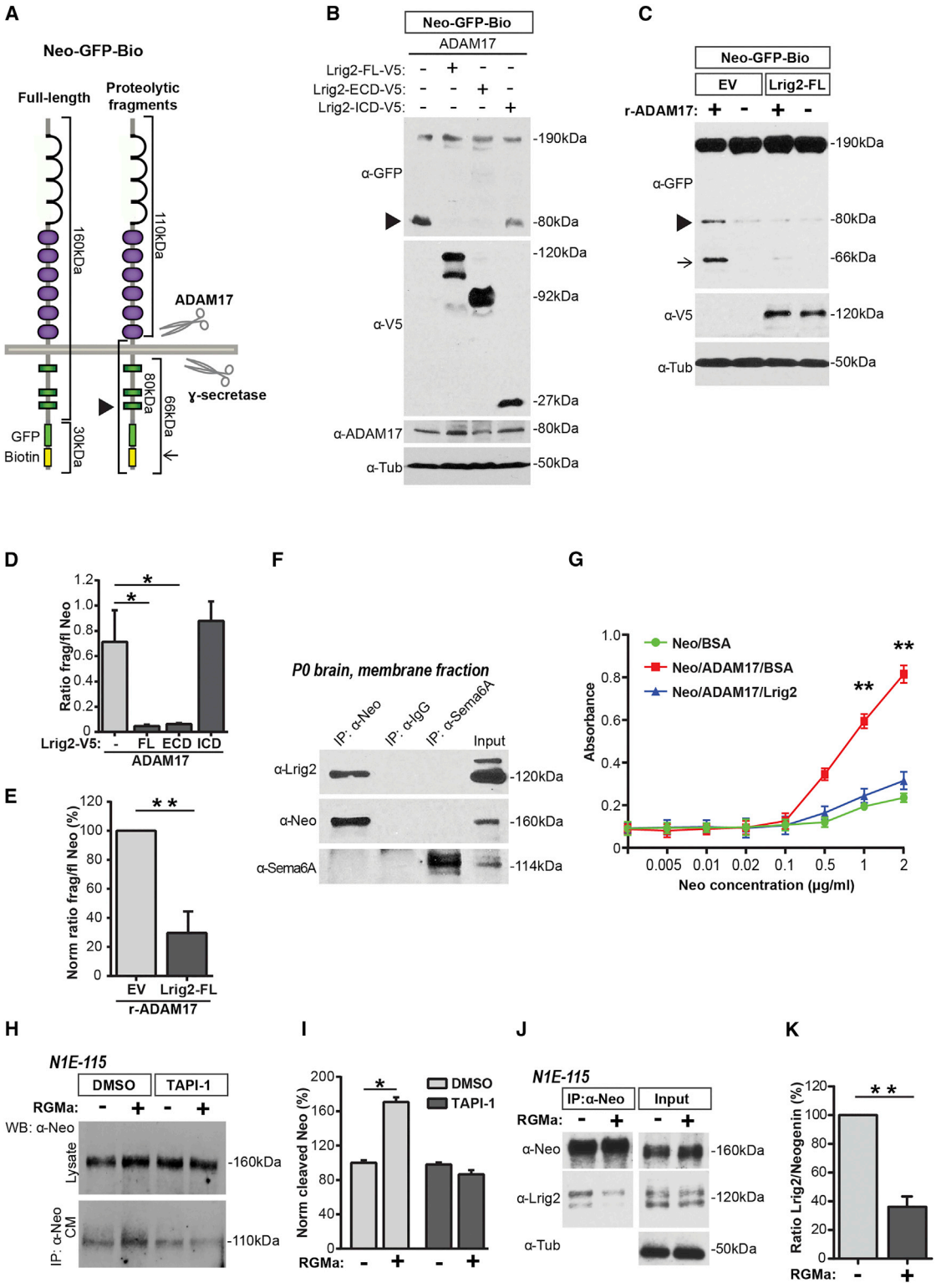

Figure 5. Lrig2 Inhibits Cleavage of Neogenin by ADAM17

(A) Neogenin can be proteolytically processed by ADAM17 and γ-secretase, leading to protein fragments of the indicated size. Arrowhead and arrow are used in (B) and (C) to indicate these fragments.

(B) Streptavidin pull-down assays on lysates of HEK293 cells co-expressing the indicated constructs together with BirA. Proteins bound to streptavidin beads were analyzed by western blotting using the indicated antibodies. ECD, extracellular domain; FL, full-length; ICD, intracellular domain.

(legend continued on next page)

confluent CHO cells in the presence of TAPI-1 or vehicle or in combination with ADAM17 knockdown. Neurons grown on CHO-RGMa cells had significantly shorter neurites, and knockdown of Lrig2 restored neurite length toward control levels. This effect of Lrig2 knockdown was rescued by treatment with TAPI-1 or by ADAM17 knockdown (Figures 6A, 6B, and S5G). These results show that regulation of ADAM17-mediated Neogenin ectodomain shedding by Lrig2 is required for neurite growth inhibition by RGMa.

Lrig2 Is Required for Cortical Neuron Migration

RGMa acts as an axon guidance protein in chick and *Xenopus*, and RGMa and Neogenin regulate neuronal migration in mice (Metzger et al., 2007; O'Leary et al., 2013). Analogous to axons, migrating neurons have a long leading process tipped by a growth cone-like structure, which detects extracellular cues. During development of the cortex, pyramidal neurons migrate from the ventricular zone (VZ) to the more superficial cortical plate (CP) to differentiate and establish functional connections (Figure 6C). Our immunohistochemical studies show that Lrig2, Neogenin, and ADAM17 are expressed in migrating cortical neurons (Figures 2 and 4). To determine the role of Lrig2 and Neogenin during cortical neuron migration, shRNA vectors together with GFP were targeted to neuronal progenitors in the VZ by in utero electroporation (IUE) at E14.5 followed by immunohistochemical characterization of the neurons that derived from these progenitors. At E16.5, scrambled control shScr^{+} neurons were primarily found in the intermediate zone (IZ) (Figure 6D). In contrast, knockdown of Lrig2 or Neogenin caused an increase in the percentage of neurons found in the VZ/subventricular zone (SVZ) and CP and a corresponding decreased percentage of neurons in the IZ. These phenotypes were not observed when shRNAs were co-electroporated with their corresponding rescue constructs (Figures 6D, 6E, and S5H). These data, coupled with *RGMa* expression in the VZ and CP (Figure S7A) and the ability of RGMa to repel migrating neurons, suggest that RGMa-Neogenin-Lrig2 signaling propels migrating neurons out of the VZ/SVZ and prevents their premature entry into the CP. To further functionally link Lrig2 and Neogenin, we combined knockdown of Lrig2 with overexpression or knockdown of Neogenin. Lrig2 knockdown triggers uncontrolled cleavage of Neogenin by ADAM17, leading to RGMa insensitivity (Figures 4, 6A, and 6B). We predicted that expression of exogenous Neogenin would restore Neogenin cell-surface expression due to the limited capacity of endogenous ADAM17 to cleave excess Neogenin. Indeed, combined transfection of shLrig2 and a Neogenin expression vector increased Neogenin cell-surface expression as compared to shLrig2 alone (Figure 6H). Furthermore, no defects in neuron migration were detected following co-electroporation of shLrig2 and Neogenin (Figures 6D and 6F). shNeo or shLrig2 induce highly similar changes in cortical neuron migration. If Lrig2 primarily acts through Neogenin in migrating neurons, then defects observed following single or combined knockdown of Lrig2 and Neogenin should to be comparable. Indeed, the percentages of ectopic cells observed following IUE of shLrig2, shNeo, or shLrig2+shNeo were similar (Figures 6D and 6F). Thus, Lrig2 acts through Neogenin to regulate cortical neuron migration.

Next, we determined the contribution of ADAM17. Knockdown of ADAM17 in dissociated cortical neurons leads to prolonged Neogenin signaling and enhanced RGMa sensitivity (Okamura et al., 2011). Neogenin knockdown induces a marked decrease in endogenous Neogenin levels, but residual Neogenin expression can usually be detected (Figure S7B). Thus, we wanted to know whether knockdown of ADAM17 could potentiate these residual Neogenin molecules and thereby partially restore the migration defects. IUE of shNeo+siADAM17 caused a small but significant decrease in the number of ectopic neurons, as compared to shNeo. siADAM17 alone mildly inhibited neuronal migration into the CP, but this effect was too small to account for the reduction in ectopic neurons observed following IUE of shNeo+siADAM17 (Figures 6D and 6G). Next, we combined knockdown of Lrig2 and ADAM17. shLrig2+siADAM17 increased Neogenin cell-surface expression in cortical neurons in vitro, while in vivo it restored the normal distribution of migrating neurons (Figures 6D, 6G, and 6H). Together, our data indicate that Lrig2 regulates ADAM17-mediated cleavage of Neogenin to control neuronal migration in the developing cortex.

Knockdown of Lrig2 Promotes CNS Axon Regeneration

RGMa contributes to the axon growth inhibitory environment of the injured mammalian CNS, and intrathecal application of RGMa antibodies promotes axon regeneration after rat spinal cord injury (Hata et al., 2006). To test whether Lrig2 manipulation

(C) Lysates of HEK293 cells transfected with the indicated constructs were incubated at 37°C with or without recombinant ADAM17 (r-ADAM17) and subjected to western blot analysis. Arrowhead indicates ADAM17-induced Neogenin fragment and arrow indicates fragment produced by γ-secretase cleavage.

(D) Quantification of band intensities as in (B). Ratio between cleaved (frag; 80 kDa) and full-length Neogenin (flNeo) was calculated. *$p < 0.05$, one-sample t test.

(E) Quantification of band intensities as in (C). Ratio between full-length and cleaved Neogenin was calculated in r-ADAM17 experiments, and data were normalized to control. **$p < 0.01$, one-sample t test.

(F) P0 mouse brain membrane fractions were subjected to immunoprecipitation with the indicated antibodies followed by western blotting. Semaphorin6A (Sema6A) was used as a negative control.

(G) ELISAs detected a concentration-dependent increase in binding of Neogenin-ECD (Neo) to wells coated with recombinant ADAM17 (Neo/ADAM17/BSA). In contrast, no significant increase in Neo binding was observed following addition of excess Lrig2 ECD (5.0 μg/ml; Neo/ADAM17/Lrig2). Lrig2 does not bind ADAM17 (data not shown). **$p < 0.01$ (Neo/ADAM17/BSA versus Neo/BSA), one-way ANOVA followed by Scheffe's multiple comparison test.

(H) N1E-115 cells were incubated with BSA control or 2 μg/ml RGMa-His with vehicle (DMSO) or TAPI-1. Western blot analysis was performed on cell lysates or on anti-Neogenin immunoprecipitates from conditioned N1E-115 cell medium (CM).

(I) Quantification of band intensities as in (H). Levels of cleaved Neogenin were normalized to control. **$p < 0.01$, Student's t test.

(J) Immunoprecipitation of Neogenin from lysates of N1E-115 cells treated with Fc control or 2 μg/ml RGMa-Fc protein. Immunoprecipitates were analyzed with the indicated antibodies.

(K) Quantification of band intensities as in (J). Ratio between Lrig2 and Neogenin bands was calculated in pull-down samples, and data were normalized to control. **$p < 0.01$, Student's t test.

All data are presented as means (of three or more independent experiments) ± SEM.

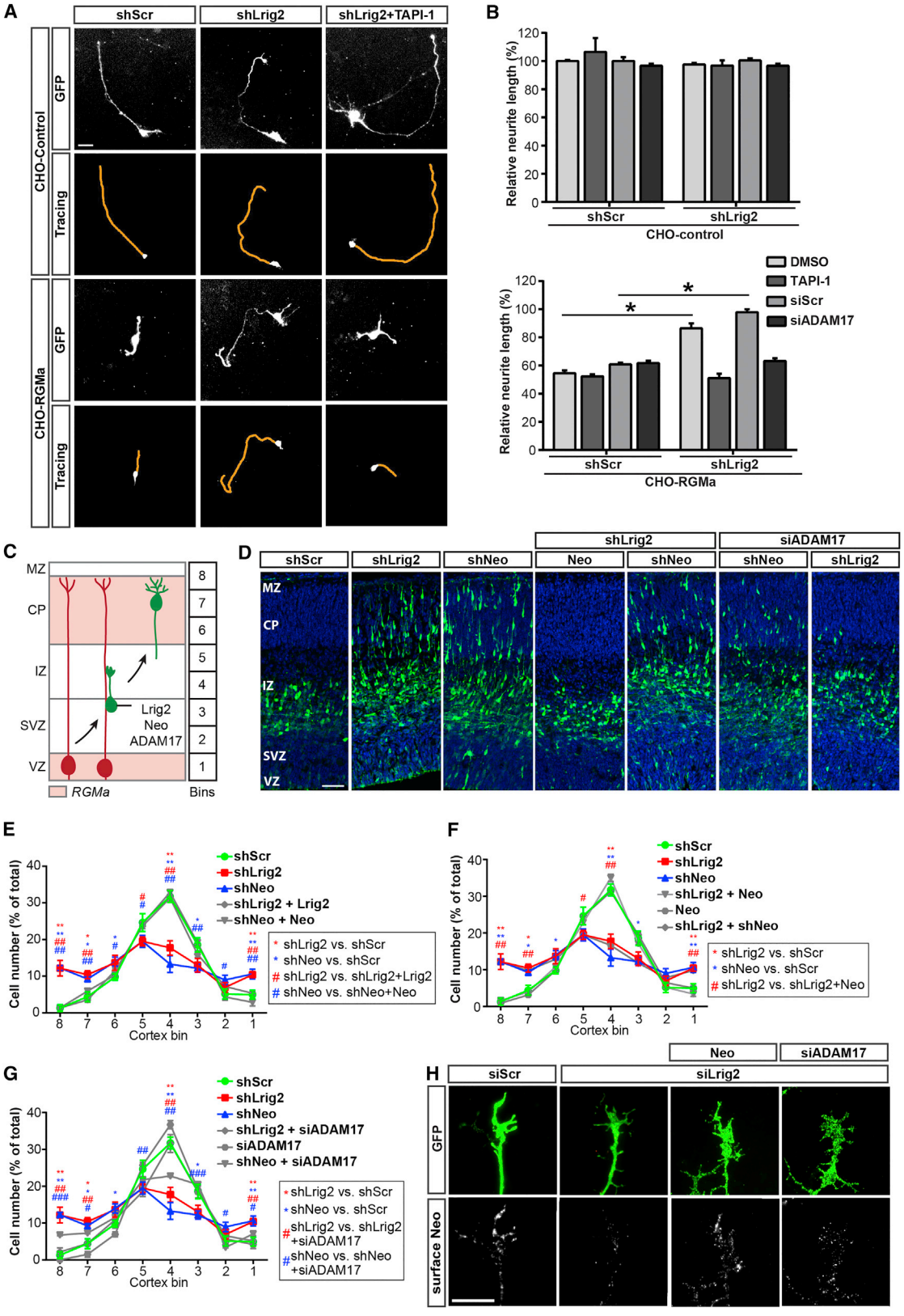

(legend on next page)

could affect axon regeneration, we used the optic nerve crush model. siRNAs can be efficiently targeted to adult retinal ganglion cells (RGCs), and optic nerve regeneration can be reliably quantified. Further, recent work shows that removal of Neogenin from lipid rafts promotes regeneration of RGC axons following optic nerve injury (ONI) (Tassew et al., 2014). We first used immunohistochemistry to detect Neogenin expression in RGCs in the uninjured adult mouse retina and at 14 days after ONI. Neogenin was found in both intact and injured RGCs (Figures 7A and 7B). Next, we induced knockdown of Neogenin in the eye by intravitreal injection of siRNAs targeting Neogenin (siNeo) in combination with ONI (Figure 7C). Following electroporation of scrambled control siRNAs, most cholera toxin subunit B (CTB)-labeled RGC axons stopped abruptly at the crush site and few fibers crossed the lesion into the distal nerve. In contrast, siNeo induced significant regeneration beyond the lesion site and more pronounced sprouting in the distal segment of the nerve (Figures 7D, 7E, and S7B). Next, we determined whether knockdown of Lrig2 in RGCs would also promote optic nerve regeneration. Immunohistochemistry revealed expression of Lrig2 in intact and injured adult mouse RGCs, and qPCR confirmed *Lrig2* knockdown efficiency following intravitreal siLrig2 injection (Figures 7B and S7C). In stark contrast to the siScr condition, knockdown of Lrig2 in RGCs with two different siRNAs induced pronounced regeneration of numerous CTB-labeled RGC axons beyond the lesion site and into the distal nerve (Figures 7D, 7F, and S7). To ask whether Lrig2 acts through Neogenin to inhibit axon regeneration, we combined siLrig2#1 with Neogenin overexpression analogous to our approach in IUE experiments (Figure 6D). Overexpression of Neogenin alone mildly inhibited axon regeneration, but this effect was too small to explain the strong reduction in siLrig2-induced axon regeneration following co-electroporation of siLrig2#1 with Neogenin (Figures 7F, S7D, and S7G). Finally, we combined knockdown of Lrig2 and ADAM17 to determine whether ADAM17 contributes to the inhibitory effect of Lrig2 on regenerating axons. Immunohistochemistry showed expression of ADAM17 in intact and injured RGCs, and qPCR confirmed *ADAM17* knockdown efficiency following intravitreal siADAM17 injection (Figures 7B, S7E, and S7F). ADAM17 knockdown had a small but significant inhibitory effect on axon regeneration by itself, but when combined with siLrig#1, it restored regeneration inhibition to control levels (Figures 7D and 7F). These data show that Lrig2 cooperates with Neogenin and ADAM17 to hamper CNS regeneration.

The observation that Neogenin overexpression can only partially inhibit the regeneration promoting effect of Lrig2 knockdown suggested that Lrig2 may regulate multiple different proteins to inhibit optic nerve regeneration. Therefore, we tested the hypothesis that Lrig2-mediated regulation of ADAM17 proteolysis is a more general mechanism. We tested the ability of Lrig2 to negatively regulate cleavage of two other ADAM17 substrates, neural cell adhesion molecule 1 (NCAM1) and Semaphorin 4D (Sema4D), after we confirmed their ability to bind Lrig2 (Figure 7G). Interestingly, cleavage of NCAM1-GFP by ADAM17 was reduced by co-expression of Lrig2 (Figure 7H). Similarly, Lrig2 reduced ADAM17-induced cleavage of FLAG-tagged Sema4D (Figure 7I). These data suggest that Lrig2 may negatively regulate the ADAM17-dependent processing of multiple, distinct cell-surface proteins.

DISCUSSION

Neural circuit development and regeneration depend on the precise regulation of guidance receptors at the plasma membrane. Different mechanisms control guidance receptor expression, including proteolysis by ADAM proteases. However, how cleavage of guidance receptors by ADAMs is spatiotemporally regulated to control receptor signaling in neurons remains incompletely understood. Here, we show that Lrig2 binds the RGMa receptor Neogenin and negatively regulates Neogenin ectodomain shedding by ADAM17. Regulation of ADAM17-mediated Neogenin shedding by Lrig2 is required for the repulsive effects of RGMa-Neogenin signaling on growing axons in vitro, and on migrating cortical neurons in vivo. Further, in line with the inhibitory effect of RGMa on axon regeneration, knockdown of Lrig2 promotes optic nerve regeneration. Together, our data unveil a unique mechanism for ADAM regulation that acts at the substrate level to control premature receptor shedding while retaining ligand responsiveness. In addition, our findings identify Lrig2 as a potential target for promoting axon regeneration.

Negative Regulation of Ectodomain Shedding by Lrig2

Shedding of guidance receptors by ADAMs regulates receptor cell-surface expression, activation of downstream signaling,

Figure 6. Regulation of ADAM17-Mediated Shedding of Neogenin by Lrig2 Controls Cortical Neuron Migration

(A and B) Dissociated E14.5 cortical neurons were electroporated with GFP vector and combinations of the indicated vectors/siRNAs and grown on confluent CHO cell layers with vehicle or TAPI-1. At DIV4, cultures were immunostained with anti-GFP antibodies. Lower panels in (A) show tracing of longest neurite in each example. Graphs in (B) show average length of the longest neurite on CHO-Control cells (upper panel) or on CHO-RGMa cells (lower panel) normalized to control (shScr on CHO-Control cells). n = 3 experiments, >75 neurons per condition per experiment. *$p < 0.05$, two-way ANOVA.

(C) Embryonic cortical neurons express Lrig2, Neogenin (Neo), and ADAM17 as they migrate along radial glia (in red) to the superficial CP. Bins used for quantification of cell migration are shown at the right. *RGMa* is expressed in the CP and VZ. MZ, marginal zone; CP, cortical plate; IZ, intermediate zone; SVZ, subventricular zone; VZ, ventricular zone.

(D) E14.5 mouse brains were in utero electroporated with GFP vector and (combinations of) the indicated DNA constructs and siRNAs. At E16.5, brains were immunostained with anti-GFP antibodies.

(E–G) Quantification of the number of GFP-positive neurons at different positions (bins) in the cortex at E16.5, two days after in utero electroporation. Color-coded symbols in boxed area besides each graph indicate significance. Statistical analyses were performed by Mann-Whitney *U* test. *$p < 0.05$; **$p < 0.01$; ***$p < 0.001$. Data represent percentage of total.

(H) Immunocytochemistry for intracellular GFP and cell-surface Neogenin expression in growth cones of E14.5 cortical neurons transfected with the indicated siRNAs and DNA vectors at 1 DIV and fixed at DIV3.

All data are presented as means (of three or more independent experiments) ± SEM. Scale bars represent 50 μm (A), 100 μm (D), and 10 μm (H). See also Figures S5 and S7.

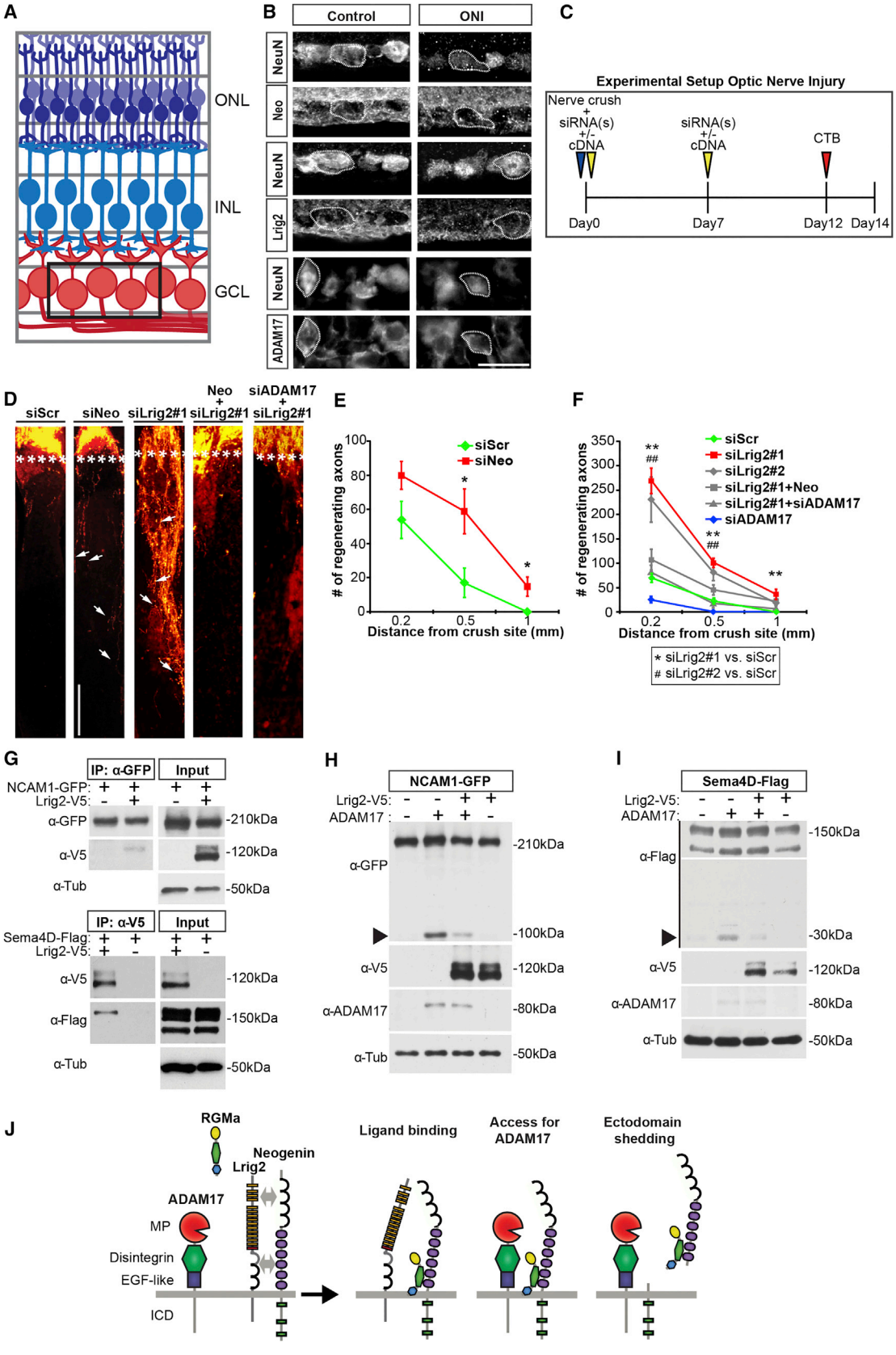

(legend on next page)

and the disassembly of ligand-receptor complexes (Bai and Pfaff, 2011). These effects require tight control of the proteolytic actions of ADAMs so as to prevent premature cleavage. Numerous molecular mechanisms have been reported for ADAM regulation in non-neuronal cell types, and these affect ADAM expression, activity, or substrates (Blobel, 2005; Scheller et al., 2011; Weber and Saftig, 2012). In contrast, much less is known about ADAM regulation in neurons. Here, we identify a unique regulatory mechanism for ADAMs by showing that Lrig2 negatively controls ADAM-mediated receptor shedding through substrate interactions in neurons. Our data indicate that Lrig2 binds Neogenin and thereby inhibits shedding of this receptor by ADAM17. Intriguingly, the Neogenin ligand RGMa dissociates the Lrig2-Neogenin complex, providing ADAM17 access to Neogenin (Figure 7J). Although our data do not formally exclude every previously reported mode of ADAM regulation, the most parsimonious explanation for our results is that binding of Lrig2 to Neogenin renders Neogenin inaccessible for cleavage in the absence of RGMa (Figure 7J).

Lrig2 Is Required for Repulsive RGMa-Neogenin Signaling

Previous work implicated ADAM17 in RGMa-Neogenin signaling by showing that this protease cleaves the Neogenin ectodomain in *cis* and thereby terminates, rather than activates, repulsive Neogenin signaling (Okamura et al., 2011). However, whether this cleavage is constitutive or tightly regulated remained unknown. Here, we show that shedding of Neogenin by ADAM17 at the growth cone is negatively controlled by Lrig2 and that this process is, at least in part, ligand dependent. We propose that this mechanism provides a way to limit premature Neogenin cleavage in the presence of active proteases while retaining immediate RGMa responsiveness. Previous work has shown that proteolysis of repulsive Ephrins by ADAM10 is also regulated by ligand-receptor binding (Hattori et al., 2000; Janes et al., 2005). Our data are, however, conceptually distinct from these previous results; we find that ligand binding induces the dissociation of a substrate inhibitor, leading to shedding, rather than inducing a new molecular recognition motif for effective cleavage.

RGMa had been reported to inhibit the migration of different types of neurons in vitro (Metzger et al., 2007; O'Leary et al., 2013). Our study confirms and extends these observations by revealing a role for RGMa-Neogenin signaling in cortical neuron migration in vivo and by demonstrating that these RGMa-induced effects rely on regulation of ADAM17-mediated Neogenin shedding by Lrig2. Although originally identified as axon repulsive cues, RGMs are now known to control a plethora of unrelated (non-)neuronal processes via Neogenin (Severyn et al., 2009). In addition, Neogenin not only binds RGMs but also functions as a cell-surface receptor for BMPs and Netrin-1 in processes such myotube formation and endochondral bone development (Kang et al., 2004; Zhou et al., 2010). Therefore, it will be important to determine whether Lrig2 regulates RGMa-Neogenin signaling events unrelated to axon growth inhibition or Neogenin signaling in response to non-RGM ligands.

Knockdown of Lrig2 Promotes Axon Regeneration in the Adult CNS

Intravitreal injections of *Lrig2* siRNAs induced significant regenerative axon growth into the distal denervated portion of the crushed optic nerve. This observation supports the exciting possibility that Lrig2 may serve as a therapeutic target for promoting axon regeneration in the injured CNS. Our data further indicate that Lrig2 normally inhibits axon regeneration by negatively regulating ADAM17. The effect of Lrig2 knockdown on axon regeneration is in line with the reported role of RGMa as an inhibitor of axon regeneration (Demicheva et al., 2015; Hata et al., 2006; Tassew et al., 2014) and with the functional requirement for Lrig2 in repulsive RGMa-Neogenin signaling. While it is tempting to speculate that knockdown of Lrig2 decreases the sensitivity of injured axons to scar-tissue-associated RGMa and thereby promotes regeneration, it should be noted that although *Neogenin* and *Lrig2* siRNAs induced a similar reduction in RGC gene expression in vivo, a far larger number of regenerating optic nerve fibers was observed following Lrig2 knockdown. Further, Neogenin overexpression following injection of Lrig2 siRNAs only partially rescued the effect of Lrig2 knockdown. A plausible explanation for this apparent discrepancy is that knockdown of Lrig2 could block the effects of multiple, distinct, regeneration-inhibiting proteins. For example, Lrig2 binds and reduces shedding of not only Neogenin but also Sema4D, a repulsive cue upregulated at CNS lesion sites (Moreau-Fauvarque et al., 2003).

Figure 7. Knockdown of Lrig2 Promotes Optic Nerve Regeneration

(A) Cell layers in the adult mouse retina. Cell bodies of retinal ganglion cells (RGCs) are located in the ganglion cell layer (GCL) and send their axons through the optic nerve to the CNS. Boxed area in the GCL indicates the region shown in (B). INL, inner nerve layer; ONL, outer nerve layer.

(B) Immunohistochemistry for Neogenin, Lrig2, or ADAM17 combined with NeuN immunostaining, to visualize RGCs, on adult mouse control retinas or at 14 days after optic nerve injury (ONI).

(C) Experimental setup of the ONI studies. siRNAs and/or pCAG-Neogenin-GFP expression vector and CTB were injected in the eye and mice were sacrificed at day 14 post-injury. CTB, Alexa Fluor-555 conjugated cholera toxin subunit B.

(D) Confocal images of optic nerve axons labeled by CTB at 14 days post-injury. Asterisks indicate the distal border of the injury site. Arrows indicate regenerating axons.

(E and F) Quantification of regenerating axons extending at specific distances from the distal end of the crush site at 14 days post-injury, as in (D). n = 6 animals per condition. *$p < 0.05$; **$p < 0.01$, Student's t test. Data are presented as means ± SEM.

(G) HEK293 cells were cotransfected with the indicated constructs followed by anti-GFP or anti-V5 pull-downs and subjected to western blot analysis.

(H and I) HEK293 cells were co-transfected with the indicated constructs and subjected to western blot analysis using the indicated antibodies. Arrowhead indicates ADAM17-induced cleavage products.

(J) In our model, Lrig2 binds Neogenin at the cell surface to prevent premature cleavage of this guidance receptor by ADAM17. Binding of RGMa induces the dissociation of the Lrig2-Neogenin complex, which provides ADAM17 with access to Neogenin, resulting in ectodomain shedding. EGF-like, epidermal growth factor-like; MP, metalloprotease.

Scale bars represent 20 μm (B) and 200 μm (D). See also Figure S7.

A General Role for Lrigs in Membrane Receptor Shedding?

Despite reported neuronal expression, how Lrigs contribute to nervous system development and function is poorly understood. Lrig1 negatively regulates glial cell-line-derived neurotrophic factor (GDNF)-induced neurite growth in vitro by binding the GDNF receptor Ret (Ledda et al., 2008). In addition, sensory innervation of the cochlea is disrupted in *Lrig1*:*Lrig2* double-knockout mice, hinting at axonal defects (Del Rio et al., 2013). Our data extend these findings by revealing a unique neuronal function for the poorly characterized Lrig family member Lrig2 and by showing that Lrigs regulate cellular responses not only to chemotrophic growth factors (e.g., EGF, GDNF) but also to chemotropic guidance cues (RGMa). This new insight is interesting in light of the identification of *LRIG2* mutations as a cause of urofacial syndrome (UFS), a congenital autosomal-recessive disorder characterized by aberrant urinary bladder innervation (Stuart et al., 2013). How UFS mutations affect Lrig2 function is unknown, but it is tempting to speculate that they impair guidance of Lrig2-positive axons that target the bladder.

Lrigs act through different molecular mechanisms to control growth factor receptors. Lrigs enhance receptor degradation, inhibit ligand-receptor interactions, and recruit receptors to lipid rafts (e.g., Gur et al., 2004; Laederich et al., 2004; Ledda et al., 2008; Wong et al., 2012). Our study demonstrates an additional level of complexity of Lrig-dependent receptor regulation by identifying Lrig2 as an inhibitor of receptor ectodomain shedding. Several growth factor receptors, such as Met and ErbB4, are Lrig binding partners and ADAM substrates (Blobel, 2005; Scheller et al., 2011). This raises the intriguing possibility that ectodomain shedding represents an additional mechanism through which Lrigs control growth factor receptors. However, our work and that of others indicate that the role of Lrigs is not restricted to growth factor receptors. In *C. elegans*, sma-10/Lrig binds BMP receptors, while Lrig3 modulates Wnt signaling in *Xenopus* (Gumienny et al., 2010; Zhao et al., 2008). Furthermore, we report here that Lrig2 inhibits shedding of several factors (Neogenin, NCAM1, and Sema4D) that serve important roles in embryonic development and immune function (Maness and Schachner, 2007; Suzuki et al., 2008) and additionally that all three Lrigs can bind Neogenin and inhibit Neogenin ectodomain shedding (Figures S7H–S7J). This wide array of Lrig binding partners with diverse functions suggests that Lrig-dependent regulation of ectodomain shedding may be a common mechanism in normal physiology and disease.

In conclusion, our findings highlight an important role for Lrigs in neurons and unveil a unique mechanism that negatively controls ADAM protease function. The regulatory mechanism described here may provide new ways to understand or manipulate other cleavage events mediated by ADAMs with roles in development, physiology, and disease.

EXPERIMENTAL PROCEDURES

Mice

Animal use and care was in accordance with institutional and national guidelines (Dierexperimentencommissie). For IUE, mouse embryos were injected with (combinations of) shRNAs, siRNAs, and DNA vectors together with pCAG-GFP. Motor cortices were targeted by electroporation with an ECM 830 Electro-Square-Porator (Harvard Apparatus) set to five unipolar pulses of 50 ms at 30 V (950-ms interval). Embryos were placed back into the abdomen, and abdominal muscles and skin were sutured separately. Embryos were collected at E16.5, and heads were fixed in 4% paraformaldehyde (PFA) and submerged in 30% sucrose. Timed-pregnant mice, optic nerve injury, and other animal procedures are described in Supplemental Experimental Procedures.

Immunolabeling, In Situ Hybridization, and Biochemical Experiments

Nonradioactive in situ hybridization and immunohistochemistry were performed as described previously (Schmidt et al., 2014). Western blotting, immunoprecipitation, and mass spectrometry were as described previously (Groen et al., 2013). For Rho pull-down assays, cells were lysed in lysis buffer followed by centrifugation at 4°C at 15,000 rpm for 10 min. To collect active Rho protein, supernatants were incubated with 50 μg GST-tagged Rho-binding domain (RBD) of rhotekin beads at 4°C for 45 min. The beads were washed four times with lysis buffer and subjected to SDS-PAGE followed by western blotting using anti- RhoA antibody. Whole-cell lysates were also subjected to western blotting for total RhoA. ELISAs were performed as described previously (Okamura et al., 2011). In brief, mouse Neogenin-ECD-Fc (0.005–2.0 μg/ml; R&D Systems) diluted in 0.1% BSA/PBS was added to 96-well ELISA microplates (Thermo Fisher Scientific) coated with 0.5 μg/ml BSA or 0.5 μg/ml recombinant ADAM17 (R&D Systems). To examine the effect of Lrig2, Neogenin-ECD-Fc was pre-incubated with 5.0 μg/ml BSA or 5.0 μg/ml Lrig2-ECD purified from HEK293 cells in PBS, before addition to ADAM17-coated ELISA plates. Two hours after incubation at room temperature, plates were washed and diluted, and anti-Neogenin (1:1,000; R&D Systems) or anti-Fc antibody (1:1,000; Sigma) was added. Horseradish peroxidase (HRP)-conjugated secondary antibodies, a substrate reagent pack, and stop solutions (R&D Systems) were used for detection. The absorbance at 450 nm was measured. To biochemically assess receptor cell-surface expression or internalization, N1E-115 cells were incubated with EZ-Link Sulfo-NHS-Biotin or EZ-Link Sulfo-NHS-SS-Biotin, respectively, and subjected to western blot analysis. For more details, please see Supplemental Experimental Procedures.

Cell Culture

Dissociated neuron cultures were prepared and transfected with siRNAs or DNA constructs as described previously (Van Battum et al., 2014). Growth cone collapse assays were performed on transfected P0 cortical neurons at 1 day in vitro using 2 μg/ml RGMa or control protein (Hata et al., 2006). For CHO cell layer assays, dissociated cortical neurons were electroporated and cultured for 4 days on confluent layers of CHO-K1 (control) or CHO-RGMa cells. For more details, please see Supplemental Experimental Procedures.

Quantification and Statistics Methods

Statistical analyses were performed using GraphPad Prism 6 software using the Student's t test or one- or two-way ANOVA followed by Dunnett's or Tukey-Kramer's test. All data were derived from at least three independently performed experiments, unless stated otherwise. Data are expressed as mean ± SEM, and significance was defined as $p < 0.05$.

SUPPLEMENTAL INFORMATION

Supplemental Information includes Supplemental Experimental Procedures, seven figures, and two tables and can be found with this article online at http://dx.doi.org/10.1016/j.devcel.2015.11.008.

AUTHOR CONTRIBUTIONS

S.v.E., D.M.A.v.d.H., and R.J.P. conceived and designed the study. Y.F. and T.Y. performed Rho signaling and optic nerve experiments. J.A.A.D. performed mass spectrometry analysis, R.A.R. and C.S. performed SPR studies, and M.K. and C.C.H. performed FRAP studies. H.H. provided unpublished reagents. All other experiments and analyses were performed by S.v.E., D.M.A.v.d.H., A.J.C.G.M.H., Y.A., E.Y.B., and A.M.B. S.v.E., D.M.A.v.d.H., and R.J.P. wrote the manuscript with input from all other authors. All authors discussed and interpreted results.

ACKNOWLEDGMENTS

We thank members of the Pasterkamp laboratory for assistance and helpful discussions and Alex Kolodkin and Joost Verhaagen for comments on the manuscript. We thank Stephen Strittmatter, Dennis Selkoe, Thomas Skutella, Atsushi Kumanogoh, and Ruud Toonen for providing antibodies and DNA constructs. This work was supported by the Netherlands Organization for Health Research and Development (ZonMW-VIDI), the Human Frontier Science Program (HFSP-CDA), Hersenstichting Nederland, Prinses Beatrix Spierfonds, the ALS Foundation (TOTALS), and Neuroscience and Cognition Utrecht to R.J.P., and a Grant-in-Aid for Scientific Research (S) from the JSPS (25221309) to T.Y. This study was partly performed within the framework of Dutch Top Institute Pharma project T5-207 and the Center for Translational Molecular Medicine (project EMINENCE, 01C-204) (to R.J.P.). R.J.P. was a Henry and William Test National Alliance for Research on Schizophrenia and Depression Investigator. R.A.R. is supported by the Medical Research Council UK (MRC) (MR/L017776/1). C.S. is a Cancer Research UK Senior Research Fellow (C20724/A14414).

Received: December 4, 2014
Revised: October 2, 2015
Accepted: November 9, 2015
Published: December 7, 2015

REFERENCES

Bai, G., and Pfaff, S.L. (2011). Protease regulation: the Yin and Yang of neural development and disease. Neuron *72*, 9–21.

Bell, C.H., Healey, E., van Erp, S., Bishop, B., Tang, C., Gilbert, R.J.C., Aricescu, A.R., Pasterkamp, R.J., and Siebold, C. (2013). Structure of the repulsive guidance molecule (RGM)-neogenin signaling hub. Science *341*, 77–80.

Blobel, C.P. (2005). ADAMs: key components in EGFR signalling and development. Nat. Rev. Mol. Cell Biol. *6*, 32–43.

Conrad, S., Genth, H., Hofmann, F., Just, I., and Skutella, T. (2007). Neogenin-RGMa signaling at the growth cone is bone morphogenetic protein-independent and involves RhoA, ROCK, and PKC. J. Biol. Chem. *282*, 16423–16433.

Del Rio, T., Nishitani, A.M., Yu, W.-M., and Goodrich, L.V. (2013). In vivo analysis of Lrig genes reveals redundant and independent functions in the inner ear. PLoS Genet. *9*, e1003824.

Demicheva, E., Cui, Y.-F., Bardwell, P., Barghorn, S., Kron, M., Meyer, A.H., Schmidt, M., Gerlach, B., Leddy, M., Barlow, E., et al. (2015). Targeting repulsive guidance molecule A to promote regeneration and neuroprotection in multiple sclerosis. Cell Rep. *10*, 1887–1898.

Goldschneider, D., Rama, N., Guix, C., and Mehlen, P. (2008). The neogenin intracellular domain regulates gene transcription via nuclear translocation. Mol. Cell. Biol. *28*, 4068–4079.

Groen, E.J.N., Fumoto, K., Blokhuis, A.M., Engelen-Lee, J., Zhou, Y., van den Heuvel, D.M.A., Koppers, M., van Diggelen, F., van Heest, J., Demmers, J.A.A., et al. (2013). ALS-associated mutations in FUS disrupt the axonal distribution and function of SMN. Hum. Mol. Genet. *22*, 3690–3704.

Gumienny, T.L., Macneil, L., Zimmerman, C.M., Wang, H., Chin, L., Wrana, J.L., and Padgett, R.W. (2010). Caenorhabditis elegans SMA-10/LRIG is a conserved transmembrane protein that enhances bone morphogenetic protein signaling. PLoS Genet. *6*, e1000963.

Guo, D., Holmlund, C., Henriksson, R., and Hedman, H. (2004). The LRIG gene family has three vertebrate paralogs widely expressed in human and mouse tissues and a homolog in Ascidiacea. Genomics *84*, 157–165.

Gur, G., Rubin, C., Katz, M., Amit, I., Citri, A., Nilsson, J., Amariglio, N., Henriksson, R., Rechavi, G., Hedman, H., et al. (2004). LRIG1 restricts growth factor signaling by enhancing receptor ubiquitylation and degradation. EMBO J. *23*, 3270–3281.

Hata, K., Fujitani, M., Yasuda, Y., Doya, H., Saito, T., Yamagishi, S., Mueller, B.K., and Yamashita, T. (2006). RGMa inhibition promotes axonal growth and recovery after spinal cord injury. J. Cell Biol. *173*, 47–58.

Hata, K., Kaibuchi, K., Inagaki, S., and Yamashita, T. (2009). Unc5B associates with LARG to mediate the action of repulsive guidance molecule. J. Cell Biol. *184*, 737–750.

Hattori, M., Osterfield, M., and Flanagan, J.G. (2000). Regulated cleavage of a contact-mediated axon repellent. Science *289*, 1360–1365.

Janes, P.W., Saha, N., Barton, W.A., Kolev, M.V., Wimmer-Kleikamp, S.H., Nievergall, E., Blobel, C.P., Himanen, J.-P., Lackmann, M., and Nikolov, D.B. (2005). Adam meets Eph: an ADAM substrate recognition module acts as a molecular switch for ephrin cleavage in trans. Cell *123*, 291–304.

Kang, J.-S., Yi, M.-J., Zhang, W., Feinleib, J.L., Cole, F., and Krauss, R.S. (2004). Netrins and neogenin promote myotube formation. J. Cell Biol. *167*, 493–504.

Kolodkin, A.L., and Pasterkamp, R.J. (2013). SnapShot: Axon guidance II. Cell *153*, 722.e1.

Laederich, M.B., Funes-Duran, M., Yen, L., Ingalla, E., Wu, X., Carraway, K.L., 3rd, and Sweeney, C. (2004). The leucine-rich repeat protein LRIG1 is a negative regulator of ErbB family receptor tyrosine kinases. J. Biol. Chem. *279*, 47050–47056.

Ledda, F., Bieraugel, O., Fard, S.S., Vilar, M., and Paratcha, G. (2008). Lrig1 is an endogenous inhibitor of Ret receptor tyrosine kinase activation, downstream signaling, and biological responses to GDNF. J. Neurosci. *28*, 39–49.

Lindquist, D., Kvarnbrink, S., Henriksson, R., and Hedman, H. (2014). LRIG and cancer prognosis. Acta Oncol. *53*, 1135–1142.

Maness, P.F., and Schachner, M. (2007). Neural recognition molecules of the immunoglobulin superfamily: signaling transducers of axon guidance and neuronal migration. Nat. Neurosci. *10*, 19–26.

Matsunaga, E., Tauszig-Delamasure, S., Monnier, P.P., Mueller, B.K., Strittmatter, S.M., Mehlen, P., and Chédotal, A. (2004). RGM and its receptor neogenin regulate neuronal survival. Nat. Cell Biol. *6*, 749–755.

Metzger, M., Conrad, S., Skutella, T., and Just, L. (2007). RGMa inhibits neurite outgrowth of neuronal progenitors from murine enteric nervous system via the neogenin receptor in vitro. J. Neurochem. *103*, 2665–2678.

Monnier, P.P., Sierra, A., Macchi, P., Deitinghoff, L., Andersen, J.S., Mann, M., Flad, M., Hornberger, M.R., Stahl, B., Bonhoeffer, F., and Mueller, B.K. (2002). RGM is a repulsive guidance molecule for retinal axons. Nature *419*, 392–395.

Moreau-Fauvarque, C., Kumanogoh, A., Camand, E., Jaillard, C., Barbin, G., Boquet, I., Love, C., Jones, E.Y., Kikutani, H., Lubetzki, C., et al. (2003). The transmembrane semaphorin Sema4D/CD100, an inhibitor of axonal growth, is expressed on oligodendrocytes and upregulated after CNS lesion. J. Neurosci. *23*, 9229–9239.

O'Leary, C., Cole, S.J., Langford, M., Hewage, J., White, A., and Cooper, H.M. (2013). RGMa regulates cortical interneuron migration and differentiation. PLoS ONE *8*, e81711.

Okamura, Y., Kohmura, E., and Yamashita, T. (2011). TACE cleaves neogenin to desensitize cortical neurons to the repulsive guidance molecule. Neurosci. Res. *71*, 63–70.

Page, M.E., Lombard, P., Ng, F., Göttgens, B., and Jensen, K.B. (2013). The epidermis comprises autonomous compartments maintained by distinct stem cell populations. Cell Stem Cell *13*, 471–482.

Powell, A.E., Wang, Y., Li, Y., Poulin, E.J., Means, A.L., Washington, M.K., Higginbotham, J.N., Juchheim, A., Prasad, N., Levy, S.E., et al. (2012). The pan-ErbB negative regulator Lrig1 is an intestinal stem cell marker that functions as a tumor suppressor. Cell *149*, 146–158.

Rajagopalan, S., Deitinghoff, L., Davis, D., Conrad, S., Skutella, T., Chedotal, A., Mueller, B.K., and Strittmatter, S.M. (2004). Neogenin mediates the action of repulsive guidance molecule. Nat. Cell Biol. *6*, 756–762.

Scheller, J., Chalaris, A., Garbers, C., and Rose-John, S. (2011). ADAM17: a molecular switch to control inflammation and tissue regeneration. Trends Immunol. *32*, 380–387.

Schmidt, E.R.E., Brignani, S., Adolfs, Y., Lemstra, S., Demmers, J., Vidaki, M., Donahoo, A.-L.S., Lilleväli, K., Vasar, E., Richards, L.J., et al. (2014). Subdomain-mediated axon-axon signaling and chemoattraction cooperate to regulate afferent innervation of the lateral habenula. Neuron *83*, 372–387.

Severyn, C.J., Shinde, U., and Rotwein, P. (2009). Molecular biology, genetics and biochemistry of the repulsive guidance molecule family. Biochem. J. *422*, 393–403.

Stuart, H.M., Roberts, N.A., Burgu, B., Daly, S.B., Urquhart, J.E., Bhaskar, S., Dickerson, J.E., Mermerkaya, M., Silay, M.S., Lewis, M.A., et al. (2013). LRIG2 mutations cause urofacial syndrome. Am. J. Hum. Genet. *92*, 259–264.

Suzuki, Y., Miura, H., Tanemura, A., Kobayashi, K., Kondoh, G., Sano, S., Ozawa, K., Inui, S., Nakata, A., Takagi, T., et al. (2002). Targeted disruption of LIG-1 gene results in psoriasiform epidermal hyperplasia. FEBS Lett. *521*, 67–71.

Suzuki, K., Kumanogoh, A., and Kikutani, H. (2008). Semaphorins and their receptors in immune cell interactions. Nat. Immunol. *9*, 17–23.

Tassew, N.G., Mothe, A.J., Shabanzadeh, A.P., Banerjee, P., Koeberle, P.D., Bremner, R., Tator, C.H., and Monnier, P.P. (2014). Modifying lipid rafts promotes regeneration and functional recovery. Cell Rep. *8*, 1146–1159.

Van Battum, E.Y., Gunput, R.-A.F., Lemstra, S., Groen, E.J.N., Yu, K.L., Adolfs, Y., Zhou, Y., Hoogenraad, C.C., Yoshida, Y., Schachner, M., et al. (2014). The intracellular redox protein MICAL-1 regulates the development of hippocampal mossy fibre connections. Nat. Commun. *5*, 4317.

Weber, S., and Saftig, P. (2012). Ectodomain shedding and ADAMs in development. Development *139*, 3693–3709.

Wong, V.W.Y., Stange, D.E., Page, M.E., Buczacki, S., Wabik, A., Itami, S., van de Wetering, M., Poulsom, R., Wright, N.A., Trotter, M.W.B., et al. (2012). Lrig1 controls intestinal stem-cell homeostasis by negative regulation of ErbB signalling. Nat. Cell Biol. *14*, 401–408.

Zhao, H., Tanegashima, K., Ro, H., and Dawid, I.B. (2008). Lrig3 regulates neural crest formation in Xenopus by modulating Fgf and Wnt signaling pathways. Development *135*, 1283–1293.

Zhou, Z., Xie, J., Lee, D., Liu, Y., Jung, J., Zhou, L., Xiong, S., Mei, L., and Xiong, W.-C. (2010). Neogenin regulation of BMP-induced canonical Smad signaling and endochondral bone formation. Dev. Cell *19*, 90–102.

Zhu, X.-J., Wang, C.-Z., Dai, P.-G., Xie, Y., Song, N.-N., Liu, Y., Du, Q.-S., Mei, L., Ding, Y.-Q., and Xiong, W.-C. (2007). Myosin X regulates netrin receptors and functions in axonal path-finding. Nat. Cell Biol. *9*, 184–192.